Title: Structural and mutational analysis of amino acid residues involved in ATP specificity of *E. coli* acetate kinase

Short title: Specificity to ATP of acetate kinase

Author names: Aya Yoshioka, Kousaku Murata, Shigeyuki Kawai *

Affiliations: Laboratory of Basic and Applied Molecular Biotechnology, Division of Food Science and Biotechnology, Graduate School of Agriculture, Kyoto University, Uji, Kyoto 611-0011, Japan

*To whom correspondence should be addressed.
Tel: +81 774 38 3768; Fax: +81 774 38 3767; E-mail: kawais@kais.kyoto-u.ac.jp.

Abstract

Acetate kinase (AK) generally utilizes ATP as a phosphoryl donor, but AK from *Entamoeba histolytica* (PPi-ehiAK) uses PPi, not ATP, and is PPi-specific. The determinants of the phosphoryl donor specificity are unknown. Here, we inferred 5 candidate amino acid residues associated with this specificity, based on structural information. Each candidate residue in *Escherichia coli* ATP-specific AK (ATP-ecoAK), which is unable to use PPi, was substituted with the respective PPi-ehiAK amino acid residue. Each variant ATP-ecoAK had an increased K_m for ATP, indicating that the 5 residues are the determinants for the specificity to ATP in ATP-ecoAK. Moreover, Asn-337 of ATP-ecoAK was shown to be particularly significant for the specificity to ATP. The 5 residues are highly conserved in 2,625 PPi-ehiAK homologs, implying that almost all organisms have ATP-dependent, rather than PPi-dependent, AK.

Key words

PPi; ATP; acetate kinase; *Entamoeba histolytica*; *Methanosarcina thermophila*

Introduction

Acetate kinase (AK) is a critical enzyme for central carbon metabolism in bacteria and archea (1). ATP-dependent AK catalyzes the phosphorylation of acetate to produce acetyl phosphate by utilizing ATP as a phosphoryl donor and also catalyzes the reverse reaction (2). This enzyme has been purified and characterized from various archaea and bacteria, including *Methanosarcina thermophila*, *Escherichia coli*, *Thermotoga maritima*, and *Lactobacillus sanfranciscensis* (3-7). The three-dimensional structure of AK of *M. thermophila* (mthAK) has been solved (8) and several key catalytic residues have been identified based on the tertiary structural information and site-directed mutagenesis (8-15).

Flower et al. have recently shown that the AK of the amitochondriate protist *Entamoeba histolytica* (PPi-ehiAK) is a novel PPi-dependent AK that phosphorylates acetate using PPi, not ATP, as a phosphoryl donor (16). The three-dimensional structure of PPi-ehiAK has been solved and the substrate-binding site of PPi-ehiAK has been compared with that of mthAK, although without a biochemical verification (17). Despite the differences in phosphoryl donor specificity, the primary sequences of AK enzymes are highly conserved (8, 17).

The significance of AK in central carbon and energy metabolism indicates the importance of understanding the determinants of the specificity of AK for phosphoryl donors (ATP and PPi). Such understanding is also important in a structural biology context, given the structural overlap between ATP and PPi (Fig. 1). In this study, we verified that PPi-ehiAK is specific for PPi, and does not

accept ATP; and that *E. coli* AK (ATP-ecoAK) is specific for ATP, and not for PPi. We then identified the amino acid determinants of the specificity to ATP of ATP-ecoAK based on a comparison of the tertiary structures of mthAK and PPi-ehiAK and the primary structures of mthAK, PPi-ehiAK, and ATP-ecoAK, combined with site-directed mutagenesis of ATP-ecoAK.

MATERIALS AND METHODS

Expression of PPi-ehiAK *PPi-ehiAK* (KEGG ID, ehi, EHI_170010) with optimized codon usage for *E. coli* was synthesized at Operon (Tokyo, Japan) (Supplementary Fig. S1). *PPi-ehiAK* was amplified by PCR using the synthesized gene as a template with primers AK_pQE_B_F (5´-TCA CCA TCA CGG ATC CAT GTC TAA TGT GCT GAT TTT C-3´, with the *Bam*HI site underlined) and AK_pQE_S_R (5´-GCT GCA GGT CGA CCC TTA AAA CTG GAA TAA TTC TTT C-3´). The PCR product was inserted into *Bam*HI/*Sma*I sites in pQE-80L with In-Fusion (Clontech, Otsu, Japan), yielding pMK3549. *E. coli* MK3648 strain was obtained by transforming *E. coli* NovaBlue (Novagen) with pMK3549 and plasmid pLysSRARE (Novagen). PPi-ehiAK is expressed as a N-terminally His-tagged protein in *E. coli* MK3648.

For expression of PPi-ehiAK, a fresh single colony of MK3648 strain that had just been transformed was inoculated into 10 mL LB medium supplemented with 100 μg/mL ampicillin, 34 μg/mL chloramphenicol, and 12.5 μg/mL tetracycline. After culturing at 37°C aerobically overnight, the culture was transferred to the same medium (250 mL) and cultured at 37°C aerobically overnight. This culture

was again transferred to the same medium (4.5 L, 500 mL in a 2.0 L Sakaguchi flask) and cultivation was continued at 37°C aerobically until A_{600} reached 0.4. Then, isopropyl-1-β-D-thiogalactopyranoside was added to 1 mM and cultivation was continued further at 37°C aerobically for 1 h.

Purification of PPi-ehiAK MK3648 cells overexpressing PPi-ehiAK were collected by centrifugation at 8,500 *g* for 10 min, suspended in 50 mL of 20 mM HEPES-NaOH (pH 7.5), and disrupted by sonication at 4°C for 15 min with an Insonator 201M (Kubota, Tokyo, Japan). After centrifugation at 20,000 *g* for 10 min, the clear supernatant was used as the cell extract containing PPi-ehiAK. This cell extract was applied to a Talon Metal Affinity Resin column (2.5×4.5 cm) (Clontech) equilibrated with 20 mM HEPES-NaOH (pH 7.5). After washing with 150 mL of 20 mM HEPES-NaOH (pH 7.5) containing 30 mM imidazole and 300 mM NaCl, PPi-ehiAK was eluted with 150 mL of 20 mM HEPES-NaOH (pH 7.5) containing 150 mM imidazole and 300 mM NaCl. The fractions containing PPi-ehiAK were combined, dialyzed against 20 mM HEPES-NaOH (pH 7.5) at 4°C overnight, and used as the purified PPi-ehiAK. If necessary, the purified enzyme was concentrated by 3-fold with a Centriprep 10K instrument (Millipore).

Expression of ATP-ecoA For expression of ATP-ecoAK (KEGG ID, ecj, Y75_p2262), *E. coli* K12 AG1 ASKA GFP-free strain (MK3814 strain), which contained plasmid pMK3814 (pCA24N carrying the *ATP-ecoAK* gene without GFP) (18) and was stored at -80°C in the presence of 17% v/v glycerol, was inoculated into 20 mL LB medium supplemented with 34 μg/mL chloramphenicol

and cultured at 37°C aerobically overnight. This culture was transferred to the same medium (700 mL, 350 mL in a 500 mL Sakaguchi flask) and cultivation was continued at 37°C aerobically until A_{600} reached 0.6. Then, isopropyl-1-β-D-thiogalactopyranoside was added to 0.1 mM and cultivation was continued at 37°C aerobically for 3 h. Purification and dialysis were conducted as described for PPi-ehiAK above, but with use of 10 mM Tris-HCl (pH 8.0) instead of 20 mM HEPES-NaOH (pH 7.5).

Expression of variant ATP-ecoAK Site-directed mutagenesis was performed using inverse PCR followed by *Dpn*I treatment using pMK3814 as a template. The variant ATP-ecoAK plasmids were confirmed by DNA sequencing. These plasmids were introduced into the *E. coli* DH5α strain and each variant ATP-ecoAK was expressed and purified as described below for ATP-ecoAK.

Assay of AK activity The AK activity in the acetyl phosphate-forming direction was assayed at 30°C using a hydroxamate assay that detects formation of acetyl phosphate (2, 19). The assay utilizes the reaction of acetyl phosphate with hydroxylamine to form acetyl hydroxamate, which forms a colored complex with trivalent iron. The reaction mixture (333 µL) comprised 10 mM phosphoryl donor, 150 mM HEPES-NaOH (pH 6.5), 200 mM potassium acetate, 10 mM $MgCl_2$, 700 mM hydroxylamine hydrochloride, with the pH adjusted to pH 6.5 with KOH just before use, and an appropriate amount of AK. The reaction was initiated by addition of AK and terminated by addition of 333 µL of 10% trichloroacetic acid, followed by addition of 333 µL of 2.5% $FeCl_3$ in 2.0 N HCl. After incubation for

5 min, the absorbance at 540 nm (A_{540}) was measured and defined as $^{1}A_{540}$. PPi (Nakalai Tesque, Kyoto, Japan) and ATP (Wako Pure Chemical) were used as phosphoryl donors. AK was diluted with 20 mM HEPES-NaOH (pH 7.5) or 10 mM Tris-HCl (pH 8.0) if required. Control reactions were conducted without a phosphoryl donor and the resultant A_{540} was defined as $^{2}A_{540}$. AK activity was calculated as ΔA_{540} ($^{1}A_{540}$ - $^{2}A_{540}$).

The AK activity in the PPi-forming direction was assayed at 30°C by detecting formation of PPi using a PPiLight™ inorganic pyrophosphate assay (Lonza, Basel, Switzerland) (20, 21). This assay utilizes the reactions of PPi with AMP to form ATP, and of luciferase producing light from the newly formed ATP. The reaction mixture (50 µL) comprised 100 mM HEPES-NaOH (pH 6.5), 20 mM potassium phosphate (Pi) (pH 7.0), 20 mM $MgCl_2$, 1.5 mM acetyl phosphate, and an appropriate amount of AK. The reaction was initiated by addition of AK and terminated by boiling for 5 min. After the reaction, 20 µL of PPiLight™ Converting Reagent was added to the reaction mixture (40 µL) with appropriate dilution with distilled water (e.g., 50-fold dilution for the PPi-ehiAK reaction). After incubation at room temperature for 30 min, 20 µL of PPiLight™ Detection Reagent was added and the mixture (60 µL) was further incubated at room temperature for 30 min. Luminescence of the mixture was then read with a 0.1 s integration time and the relative luminescent unit (RLU) value was measured as ^{1}RLU. Control reactions were conducted without AK and the resultant RLU was defined as ^{2}RLU. AK activity in the PPi-forming direction was calculated as ΔRLU (^{1}RLU – ^{2}RLU) using an authentic PPi as a standard.

One unit (U) of enzyme activity was defined as 1 µmol acetyl phosphate

produced in 1 min at 30°C and specific activity was expressed in U/mg protein. Protein concentrations were determined by the method of Bradford (22) with bovine serum albumin as a standard.

Differential scanning fluorimetry (DSF) Interaction between AK and substrate (ATP or PPi) was assessed by DSF (23) using a MyiQ2 real-time PCR instrument (Bio-Rad). The fluorescence of SYPRO Orange (Invitrogen) was monitored using filters provided with the PCR instrument (excitation at 492 nm and emission at 610 nm). The reaction mixture (20 µl) comprised 5 µg AK, 20 mM Tris-HCl (pH 7.5), 1000-fold diluted SYPRO Orange, and each substrate (1.0 mM ATP, 5.0 mM PPi). This mixture was subjected to a temperature increase from 20 to 95°C by 0.5°C/cycle for a total of 141 cycles. The fluorescence profile was obtained by plotting the relative fluorescence unit (RFU) value at each temperature. The profile was analyzed using *iQ5* (Bio-Rad) and the midpoint of the increase in the profile was defined as the melting temperature (T_m).

Elution of AKs from an ATP-agarose column Purified ATP-ecoAK in 10 mM Tris-HCl (pH 8.0) containing 10 mM $MgCl_2$ (500 µL, 1.0 mg/mL) was applied to an ATP-agarose column (100 µL) (Sigma-Aldrich) equilibrated with 10 mM Tris-HCl (pH 8.0) containing 10 mM $MgCl_2$. The column was allowed to stand for 1 h at 4°C for binding to take place. After incubation, the column was washed with 2 mL of 10 mM Tris-HCl (pH 8.0) containing 10 mM $MgCl_2$. Next, 500 µL of 50 mM ATP (pH 7.0) containing 10 mM $MgCl_2$ was added and the column was incubated for 30 min at 4°C, followed by elution of ATP-ecoAK. In

the case of purified PPi-ehiAK in 20 mM HEPES-NaOH (pH 7.5) containing 10 mM $MgCl_2$ (500 μL, 1.0 mg/mL), the application, washing, and elution procedures were the same as those for ATP-ecoAK, but with use of 20 mM HEPES-NaOH (pH 7.5) instead of 10 mM Tris-HCl (pH 8.0).

SDS-PAGE SDS-PAGE was performed on 12.5% acrylamide gels.(24) Proteins in the gel were visualized with Coomassie brilliant blue R-250.

RESULTS

Purification and phosphoryl donor specificity of PPi-ehiAK and ATP-ecoAK An *PPi-ehiAK* gene with optimized codon usage for *E. coli* was synthesized (Fig. S1), cloned in pQE-80L, and expressed as a N-terminally His-tagged protein in *E. coli*. The purified PPi-ehiAK protein was 44 kDa on SDS-PAGE, in agreement with the calculated molecular mass (44 kDa; His-tag, 1 kDa + PPi-ehiAK, 43 kDa) (Fig. S2). Kinetic constants showed that the purified PPi-ehiAK utilized PPi, but not ATP, as a phosphoryl donor (Table 1). Native ATP-ecoAK purified from *E. coli* utilizes ATP (7), but the strict phosphoryl donor specificity of ATP-ecoAK is unknown. To examine this issue, a N-terminally His-tagged ATP-ecoAK was also expressed in *E. coli*. The purified ATP-ecoAK was shown to be specific for ATP, and not to use PPi as a phosphoryl donor (Table 1).

Candidates for determinants of the phosphoryl donor specificity of AK

To probe the structural determinants of the phosphoryl donor specificity of AK, we inspected the substrate-binding site of the tertiary structure of mthAK complexed with acetate and ADP-AlF_3 (9). Noted that although mthAK utilizes ATP for the phosphorylation of acetate (5), if mthAK uses PPi or not has not been experimentally confirmed. We found 12 residues located within 4.0 Å of ADP: Leu-209, Gly-210, Asn-211, Asp-283, Phe-284, Arg-285, Ala-330, Gly-331, Ile-332, Asn-335, Ser-336, and Arg-362. Among these residues, 5 (Asn-211, Ala-330, Gly-331, Ile-332, and Asn-335 of mthAK) are conserved in ATP-ecoAK, but not in PPi-ehiAK, based on a multiple sequence alignment (Fig. 2). This suggests that these residues are candidates for determinants of the phosphoryl donor specificity. Four of these 5 residues (Asn-211, Gly-331, Ile-332, and Asn-335) form hydrogen bonds and van der Waals contacts to ADP (Table S1). Of the other 7 residues among the original 12 in mthAK, two (Ser-336 and Arg-362) are not conserved and 5 (Leu-209, Gly-210, Asp-283, Phe-284, and Arg-285) have defined roles (8, 12) and are conserved in both ATP-ecoAK and PPi-ehiAK (Fig. 2).

Among the 5 candidate residues, Asn-211, Gly-331, and Ile-332 of mthAK have been proposed to bind to the β-phosphate, α-phosphate, and adenine base of ADP, respectively, although this has not been confirmed experimentally (Fig. 3) (8). Ala-330 is located close to the β-phosphate and Asn-335 interacts with the adenine base of ADP (Table S1), suggesting that Ala-330 and Asn-335 are key residues in recognition of ATP in mthAK (Fig. 3). Superposition of the substrate-binding site of the tertiary structure of mthAK complexed with acetate and ADP-AlF_3 (9) and that of PPi-ehiAK (17) showed that the corresponding 5

residues in PPi-ehiAK would occlude the ATP-binding cleft of mthAK and thus could reject binding of ATP to PPi-ehiAK (Fig. 3). Consistent with this observation, Gln-323 and Met-324 of PPi-ehiAK have previously been proposed to occlude the ATP-binding cleft (17).

Kinetic analyses of variant ATP-ecoAKs The candidate residues in mthAK/ATP-ecoAK/PPi-ehiAK are Asn-211/Asn-213/Thr-201, Ala-330/Gly-332/Asp-322, Gly-331/Gly-333/Gln-323, Ile-332/Ile-334/Met-324, and Asn-335/Asn-337/Glu-327 (Figs. 2 and 3). To examine the roles of these residues in phosphoryl donor specificity, each candidate residue in ATP-ecoAK, which is specific for ATP (Table 1), was substituted with the respective PPi-ehiAK residue and the variant ATP-ecoAKs were purified (Fig. S2). All 5 variant ATP-ecoAKs exhibited increased K_m and decreased V_{max} for ATP (Table 1), indicating that these residues are the determinants for the specificity to ATP in ATP-ecoAK. Notably, K_m for ATP of ATP-ecoAK N337E increased 46-fold relative to ATP-ecoAK, showing a critical role of ATP-ecoAK Asn-337 in ATP binding. Thus, Glu-327 of PPi-ehiAK may be a particularly potent determinant of rejection of ATP and promotion of PPi specificity in PPi-ehiAK (Fig. 3, Table 1). Each variant ATP-ecoAK showed no PPi-dependent AK activity for both acetyl phosphate and PPi formation (Tables 1 and S2).

Analyses of substrate binding to AKs Affinities of PPi-ehiAK, ATP-ecoAK, and variant ATP-ecoAKs for each ATP and PPi were analyzed using DSF based on changes in protein stability upon ligand binding (23). The fluorescence of SYPRO

Orange bound to denatured proteins was measured during heat treatment from 25 to 95°C. T_m values of AKs in the absence and presence of substrates were determined as the midpoint of the increase in the fluorescence profile (Table 2). The difference in T_m of native ATP-ecoAK in the presence and absence of ATP ($\Delta T_{m\ ATP}$) was 13°C, suggesting that the thermal stability of ATP-ecoAK was increased by the binding of ATP. In contrast, $\Delta T_{m\ ATP}$ of PPi-ehiAK could not be measured, concordant with the absence of ATP-dependent activity of PPi-ehiAK (Table 1). $\Delta T_{m\ ATP}$ of all variant ATP-ecoAKs was decreased significantly relative to that of native ATP-ecoAK, in agreement with the decreased activity of variant ATP-ecoAK and supporting the roles of the 5 residues as determinants of specificity for ATP. The reason for the greatly decreased $\Delta T_{m\ ATP}$ for ATP-ecoAK G332D remains to be clarified.

To confirm the ATP-binding data, ATP-ecoAK, ATP-ecoAK N337E, and PPi-ehiAK were added to an ATP-agarose column, washed, and eluted with 50 mM ATP containing 10 mM $MgCl_2$. As expected, ATP-ecoAK was eluted by ATP after complete washing, while PPi-ehiAK was not eluted (Fig. S3), in agreement with the absence of ATP-dependent activity of PPi-ehiAK and the DSF results (Tables 1 and 2). Slight elution occurred for ATP-ecoAK N337E (Fig. S3), which had a significantly increased K_m for ATP (Table 1). This confirms that the affinity of ATP-ecoAK N337E for ATP was decreased by substitution of Asn-337 to Glu.

$\Delta T_{m\ PPi}$ of PPi-ehiAK was 1.7, indicating the expected binding of PPi to PPi-ehiAK (Table 2). Unexpectedly, $\Delta T_{m\ PPi}$ of ATP-ecoAK was 4.4, suggesting that PPi can bind to ATP-ecoAK, although ATP-ecoAK cannot utilize PPi as a phosphoryl donor for catalysis (Table 1). $\Delta T_{m\ PPi}$ of ATP-ecoAK was not markedly

reduced upon substitution of each candidate residue, especially Gly-333, Ile-334, and Asn-337, compared to the effects on $\Delta T_{m\ ATP}$ (Table 2). This may reflect the role of these residues in binding to adenosine of ADP, and thus not to PPi (Fig. 3). Substitution of Asn-213 or Gly-332 of ATP-ecoAK reduced $\Delta T_{m\ PPi}$ of ATP-ecoAK. This is in agreement with the putative binding of Asn-213 of ATP-ecoAK to the ß-phosphate of ADP and putative equivalent binding of Asn-211 of mthAK to the PPi moiety. Gly-322 of ATP-ecoAK is located close to the ß-phosphate of ADP, and Ala-330 of mthAK may similarly be located close to PPi (Fig. 3).

Asn-213 and Gly-332 of ATP-ecoAK correspond to Thr-201 and Asp-322 of PPi-ehiAK respectively (Figs. 2 and 3). To examine the involvement of Thr-201 and Asp-322 of PPi-ehiAK in utilization of PPi, we focused on the residues (Leu-326 and Asn-376) of PPi-ehiAK that interact with Thr-201 and Asp-322 (Table S3, Fig. S4). Leu-326 and Asn-376 of PPi-ehiAK correspond to Glu-336 and Thr-385 of ATP-ecoAK. Glu-336, Thr-385, Asn-213 and Gly-332 of ATP-ecoAK were substituted with the respective PPi-ehiAK residues (Leu-326, Asn-376, Thr-201, and Asp-322) to give a quadruple ATP-ecoAK variant (ATP-ecoAK N213T G332D E336L T385N) that had the possibility of utilizing PPi (Fig. S2). However, this variant could not utilize PPi and $\Delta T_{m\ PPi}$ was not increased by these substitutions. V_{max} and k_{cat} for ATP were significantly decreased in the quadruple variant (Table 1) and $\Delta T_{m\ ATP}$ was markedly decreased (Table 2).

DISCUSSION

The results of the study show that PPi-ehiAK is specific for PPi and does not utilize ATP (16), while ATP-ecoAK is specific for ATP and does not use PPi. Based on the tertiary and primary structures and catalytic and binding activities of variant enzymes, we identified 5 residues (Asn-213, Gly-332, Gly-333, Ile-334, and Asn-337 in ATP-ecoAK) as determinants of specificity to ATP in ATP-ecoAK.

ATP-ecoAK N337E exhibited a 46-fold increase in K_m for ATP relative to ATP-ecoAK, indicating that Asn-337 of ATP-ecoAK is the most crucial for the specificity to ATP and suggesting that the corresponding Asn-335 in mthAK is also crucial for binding to ATP and that the corresponding Glu-327 in PPi-ehiAK is possibly important for rejection of ATP in PPi-ehiAK. The basis of the role of Asn-337 of ATP-ecoAK in accepting ATP was examined using molecular and electrostatic surfaces of the ADP-binding sites of mthAK N335E and mthAK, for which a tertiary structure has been solved (9). The ADP-binding cleft is negatively charged in mthAK N335E, but positively charged in mthAK (Fig. S5). There was no clear structural change in the molecular surface of mthAK N335E that could have resulted in rejection of ATP. Thus, the negatively charged ATP-binding site in ATP-ecoAK N337E may explain the weaker affinity for ATP.

To get further insight into the substrate specificity of AKs, we examined how the 5 key residues are distributed in the primary structures of AKs. A total of 2,625 proteins homologous to PPi-ehiAK from all species with sequenced genomes were found using BLASTP (25). Among the homologs, the 5 key residues of mthAK/ATP-ecoAK/PPi-ehiAK (Asn-211/Asn-213/Thr-201, Ala-330/Gly-332/Asp-322, Gly-331/Gly-333/Gln-323, Ile-332/Ile-334/Met-324, and Asn-335/Asn-337/Glu-327) are highly conserved as Asn, Ala or Gly, Gly, Ile,

and Asn, respectively (Table 3). These are mthAK- and ATP-ecoAK-specific residues, which suggests that almost all organisms have ATP-dependent AKs. In contrast, 10 PPi-ehiAK homologs, including PPi-ehiAK, possess the PPi-ehiAK-specific residue (Glu) in the most crucial position determining the phosphoryl donor specificity (corresponding to Asn-335/Asn-337/Glu-327 in mthAK/ATP-ecoAK/PPi-ehiAK) (Table 3). However, except for PPi-ehiAK and the PPi-ehiAK homolog from *Entamoeba dispar*, which is closely related to *E. histolytica*, 8 of these homologs have no PPi-ehiAK-specific residues in the other 4 positions (corresponding to Thr-201, Asp-322, Gln-323, and Met-324 in PPi-ehiAK) (Table S4). This suggests that only the PPi-ehiAK homolog from *E. dispar* is PPi-dependent. The phosphoryl donor specificities of the other 8 PPi-ehiAK homologs remain to be clarified.

ACKNOWLEDGEMENTS

We thank the National Bio Resource Project (NIG, Japan) for providing the *E. coli* K12 AG1 ASKA GFP-free strain. This work was partially supported by the Funding Program for Next Generation World-Leading Researchers (to S. K.).

REFERENCES

1. **Thauer, R. K., Moller-Zinkhan, D., and Spormann, A. M.:** Biochemistry of acetate catabolism in anaerobic chemotrophic bacteria, Annu. Rev. Microbiol., **43**, 43-67 (1989).
2. **Rose, I. A.:** Acetate kinase of bacteria (acetokinase), Methods. Enzymol., **1**, 591-595 (1955).
3. **Matsuyama, A., Yamamoto, H., and Nakano, E.:** Cloning, expression, and nucleotide sequence of the *Escherichia coli* K-12 *ackA* gene, J. Bacteriol., **171**, 577-580 (1989).
4. **Knorr, R., Ehrmann, M. A., and Vogel, R. F.:** Cloning, expression, and characterization of acetate kinase from *Lactobacillus sanfranciscensis*, Microbiol. Res., **156**, 267-277 (2001).
5. **Aceti, D. J., and Ferry, J. G.:** Purification and characterization of acetate kinase from acetate-grown *Methanosarcina thermophila*. Evidence for regulation of synthesis, J. Biol. Chem., **263**, 15444-15448 (1988).
6. **Bock, A. K., Glasemacher, J., Schmidt, R., and Schonheit, P.:** Purification and characterization of two extremely thermostable enzymes, phosphate acetyltransferase and acetate kinase, from the hyperthermophilic eubacterium *Thermotoga maritima*, J. Bacteriol., **181**, 1861-1867 (1999).
7. **Fox, D. K., and Roseman, S.:** Isolation and characterization of homogeneous acetate kinase from *Salmonella typhimurium* and *Escherichia coli*, J. Biol. Chem., **261**, 13487-13497 (1986).

8. **Buss, K. A., Cooper, D. R., Ingram-Smith, C., Ferry, J. G., Sanders, D. A., and Hasson, M. S.:** Urkinase: Structure of acetate kinase, a member of the ASKHA superfamily of phosphotransferases, J. Bacteriol., **183**, 680-686 (2001).

9. **Gorrell, A., Lawrence, S. H., and Ferry, J. G.:** Structural and kinetic analyses of arginine residues in the active site of the acetate kinase from *Methanosarcina thermophila*, J. Biol. Chem., **280**, 10731-10742 (2005).

10. **Ingram-Smith, C., Barber, R. D., and Ferry, J. G.:** The role of histidines in the acetate kinase from *Methanosarcina thermophila*, J. Biol. Chem., **275**, 33765-33770 (2000).

11. **Ingram-Smith, C., Gorrell, A., Lawrence, S. H., Iyer, P., Smith, K., and Ferry, J. G.:** Characterization of the acetate binding pocket in the *Methanosarcina thermophila* acetate kinase, J. Bacteriol., **187**, 2386-2394 (2005).

12. **Miles, R. D., Iyer, P. P., and Ferry, J. G.:** Site-directed mutational analysis of active site residues in the acetate kinase from *Methanosarcina thermophila*, J. Biol. Chem., **276**, 45059-45064 (2001).

13. **Miles, R. D., Gorrell, A., and Ferry, J. G.:** Evidence for a transition state analog, MgADP-aluminum fluoride-acetate, in acetate kinase from *Methanosarcina thermophila*, J. Biol. Chem., **277**, 22547-22552 (2002).

14. **Singh-Wissmann, K., Ingram-Smith, C., Miles, R. D., and Ferry, J. G.:** Identification of essential glutamates in the acetate kinase from *Methanosarcina thermophila*, J. Bacteriol., **180**, 1129-1134 (1998).

15. **Singh-Wissmann, K., Miles, R. D., Ingram-Smith, C., and Ferry, J. G.:**

Identification of essential arginines in the acetate kinase from *Methanosarcina thermophila*, Biochemistry (Mosc). **39**, 3671-3677 (2000).

16. **Fowler, M. L., Ingram-Smith, C., and Smith, K. S.:** Novel pyrophosphate-forming acetate kinase from the protist *Entamoeba histolytica*, Eukaryot. Cell, **11**, 1249-1256 (2012).

17. **Thaker, T. M., Tanabe, M., Fowler, M. L., Preininger, A. M., Ingram-Smith, C., Smith, K. S., and Iverson, T. M.:** Crystal structures of acetate kinases from the eukaryotic pathogens *Entamoeba histolytica* and *Cryptococcus neoformans*, J. Struct. Biol., **181**, 185-189 (2013).

18. **Kitagawa, M., Ara, T., Arifuzzaman, M., Ioka-Nakamichi, T., Inamoto, E., Toyonaga, H., and Mori, H.:** Complete set of ORF clones of *Escherichia coli* ASKA library (a complete set of *E. coli* K-12 ORF archive): unique resources for biological research, DNA Res., **12**, 291-299 (2005).

19. **Lipmann, F., and Tuttle, L. C.:** A specific micromethod for the determination of acyl phosphates, J. Biol. Chem., **159**, 21-28 (1945).

20. **Ghetta, A., Matus-Ortega, M., Garcia-Mena, J., Deho, G., Tortora, P., and Regonesi, M. E.:** Polynucleotide phosphorylase-based photometric assay for inorganic phosphate, Anal. Biochem., **327**, 209-214 (2004).

21. **Eriksson, J., Karamohamed, S., and Nyren, P.:** Method for real-time detection of inorganic pyrophosphatase activity, Anal. Biochem., **293**, 67-70 (2001).

22. **Bradford, M. M.:** Rapid and sensitive method for quantitation of

microgram quantities of protein utilizing principle of protein-dye binding, Anal. Biochem., **72**, 248-254 (1976).

23. **Niesen, F. H., Berglund, H., and Vedadi, M.:** The use of differential scanning fluorimetry to detect ligand interactions that promote protein stability, Nat. Protoc., **2**, 2212-2221 (2007).

24. **Laemmli, U. K.:** Cleavage of structural proteins during the assembly of the head of bacteriophage T4, Nature, **227**, 680-685 (1970).

25. **Altschul, S. F., Madden, T. L., Schaffer, A. A., Zhang, J., Zhang, Z., Miller, W., and Lipman, D. J.:** Gapped BLAST and PSI-BLAST: a new generation of protein database search programs, Nucleic. Acids. Res., **25**, 3389-3402 (1997).

26. **Kaminuma, E., Mashima, J., Kodama, Y., Gojobori, T., Ogasawara, O., Okubo, K., Takagi, T., and Nakamura, Y.:** DDBJ launches a new archive database with analytical tools for next-generation sequence data, Nucleic. Acids. Res., **38**, D33-38 (2010).

FIGURES

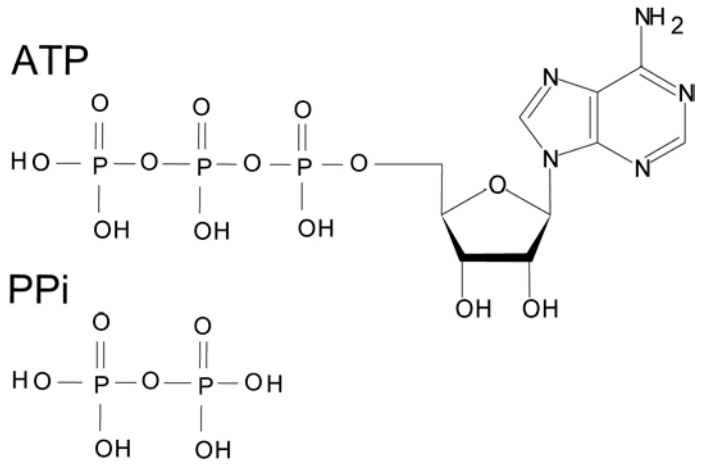

Fig. 1. Structures of ATP and PPi.

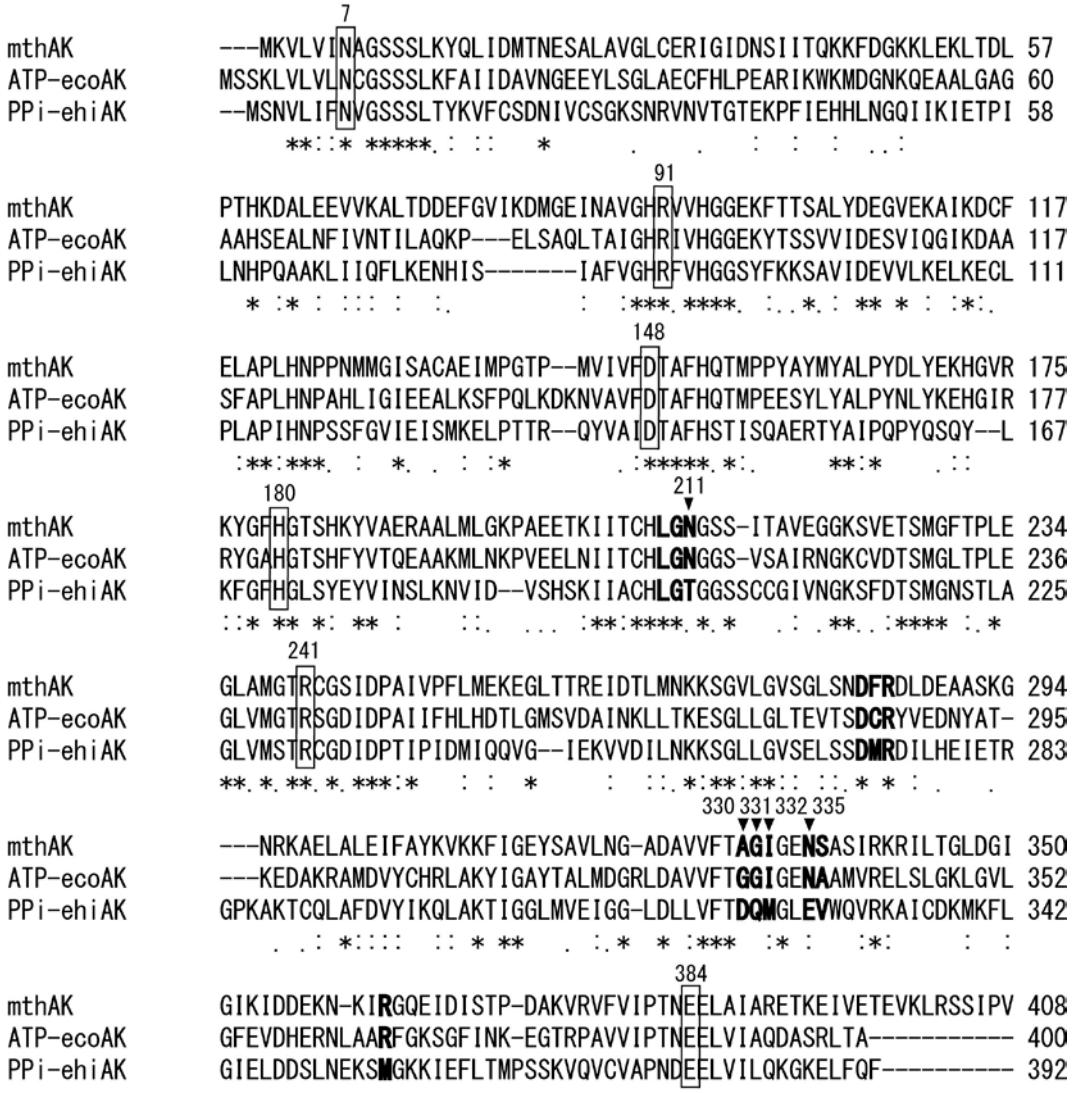

436

437 **Fig. 2.** Multiple alignment of the primary sequences of mthAK, ATP-ecoAK, and
438 PPi-ehiAK. Multiple alignment of the mthAK (Uniprot, P38502), ATP-ecoAK
439 (KEGG, Y75_p2262), and PPi-ehiAK (KEGG, EHI_170010) sequences was
440 conducted using ClustalW2 (26). The 12 residues located within 4.0 Å of ADP in
441 the tertiary structure of mthAK complexed with acetate and ADP-AlF_3 (9) are
442 shown in bold. Among these 12 residues, the 5 candidate residues for
443 determination of phosphoryl donor specificity are denoted by arrowheads. Key
444 residues involved in catalysis in mthAK (Asn-7, Arg-91, Asp-148, His-180,
445 Arg-241, and Glu-384) (8-10) are conserved in ATP-ecoAK and PPi-ehiAK and

are boxed. Identical residues are denoted by an asterisk (*), strongly conserved residues by a colon (:), and weakly conserved residues by a period (.). Numbers above the sequences refer to mthAK and numbering for each protein is shown on the right.

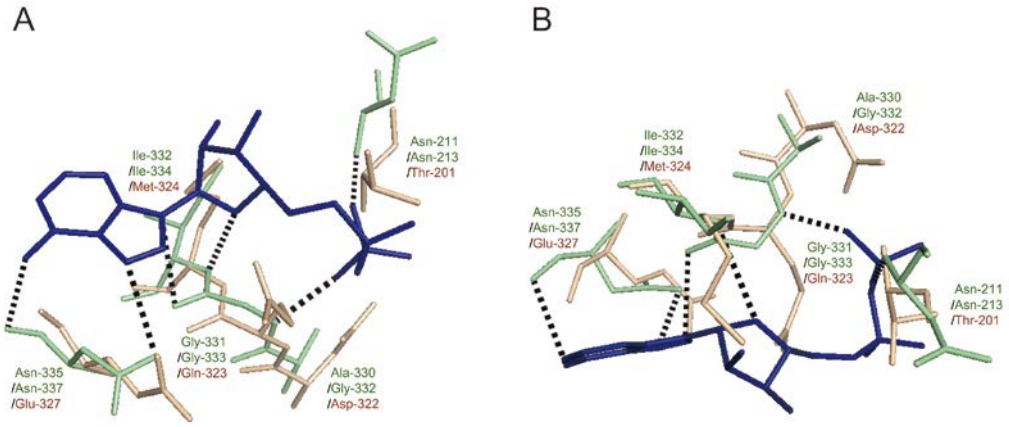

Fig. 3. Superposition of the substrate-binding site structures of mthAK and PPi-ehiAK. A, Superposition of the substrate-binding sites of PPi-ehiAK (PDB, 4H0O) (17) and mthAK complexed with acetate and ADP-AlF_3 (PDB, 1TUY) (9). Amino acid residues of mthAK are shown in green, ADP in mthAK is in deep blue, and PPi-ehiAK is in light orange. Residue names and numbers are shown as mthAK (green)/ATP-ecoAK (green)/PPi-ehiAK (pink). Hydrogen bonds in mthAK are shown as dashed lines. B, Overhead view of *A*. Superposition of AKs was performed using PyMOL.

Table 1. Kinetic constants of AKs.[a]

Phosphoryl donor	PPi			ATP		
	K_m (mM)	V_{max} (U/mg)	k_{cat} (s^{-1})	K_m (mM)	V_{max} (U/mg)	k_{cat} (s^{-1})
PPi-ehiAK	3.3 ± 0.5	3.7 ± 0.2	2.6 ± 0.1	nd	nd	nd
ATP-ecoAK	nd [b]	nd	nd	0.67 ± 0.06	1258 ± 28	908 ± 20
ATP-ecoAK N213T	nd	nd	nd	1.7 ± 0.2	22.7 ± 1.1	16.3 ± 0.8
ATP-ecoAK G332D	nd	nd	nd	3.5 ± 0.4	13.7 ± 0.7	9.9 ± 0.5
ATP-ecoAK G333Q	nd	nd	nd	5.2 ± 0.4	56.8 ± 1.5	41.0 ± 1.1
ATP-ecoAK I334M	nd	nd	nd	6.6 ± 0.6	72.8 ± 3.3	10.5 ± 0.5
ATP-ecoAK N337E	nd	nd	nd	30.7 ± 1.9	537 ± 24	395 ± 18
ATP-ecoAK N213T G332D E336L T385N	nd	nd	nd	0.66 ± 0.18	0.47 ± 0.01	0.34 ± 0.01
PPi-ehiAK [c]	3.6 ± 0.1	nr	nr	nr	nr	nr
ATP-ecoAK [d]	nr	nr	nr	0.07	2,000	nr

[a] AK activity was assayed with different concentrations of PPi or ATP. nd, not detected. nr, not reported. Kinetic values were calculated by fitting data to the appropriate Michaelis-Menten equations using KaleidaGraph software (Synergy Software). [b] ΔA_{540} was 0.11 in the presence of 5 mM PPi with 15.8 μg of PPi-ehiAK after a 10 min reaction, but ΔA_{540} was zero in the presence of 10 mM PPi with 20 μg of ATP-ecoAK, ATP-ecoAK N213T, ATP-ecoAK G332D, ATP-ecoAK G333Q, ATP-ecoAK I334M and ATP-ecoAK N337E after 10, 30 and

60 min; thus AK activities of ATP-ecoAK and variant ATP-ecoAK toward PPi were regarded as not detected (nd). ΔA_{540} was 0.036 in the presence of 10 mM ATP with 6.4×10^{-3} μg of ATP-ecoAK after a 10 min reaction, but ΔA_{540} was zero in the presence of 5 mM ATP with 15.8 μg of PPi-ehiAK after 10, 30 and 60 min; thus AK activities of PPi-ehiAK toward ATP were regarded as not detected. [c] Data from a previous report (16). [d] Data from a previous report (7).

Table 2. Differences in T_m of AKs in the absence and presence of ATP and PPi.

Enzyme	$\Delta T_{m\ ATP}$ (°C)	$\Delta T_{m\ PPi}$ (°C)
PPi-ehiAK	nd	1.7 ± 0.2
ATP-ecoAK	12.5 ± 0.9	4.4 ± 0.6
ATP-ecoAK N213T	1.9 ± 0.1	1.7 ± 0.6
ATP-ecoAK G332D	0.22 ± 0.18	2.0 ± 0.1
ATP-ecoAK G333Q	2.7 ± 0.1	3.7 ± 0.2
ATP-ecoAK I334M	1.3 ± 0.2	3.3 ± 0.2
ATP-ecoAK N337E	1.0 ± 0.1	3.4 ± 0.3
ATP-ecoAK N213T G332D E338L T385N	0.73 ± 0.20	2.7 ± 0.2

Differences in T_m of AKs in the absence and presence of ATP and PPi ($\Delta T_{m\ ATP}$ and $\Delta T_{m\ PPi}$) are shown. ATP was used at 1.0 mM and PPi at 5.0 mM. Means and standard deviations of three independent experiments are shown. nd, not detected.

Table 3. Distribution of the 5 candidate residues in AK sequences in a database search.[a]

Candidate residues of mthAK/ATP-ecoAK/PPi-ehiAK	mthAK/ATP-ecoAK-specific residues	PPi-ehiAK-specific residues
Asn-211/Asn-213/Thr-201	Asn (2,100/80%) [b]	Thr (2/0.08%)
Ala-330/Gly-332/Asp-322	Ala or Gly (2,584/98%)	Asp (3/0.11%)
Gly-331/Gly-333/Gln-323	Gly (2,581/98%)	Gln (2/0.08%)
Ile-332/Ile-334/Met-324	Ile (1,752/67%)	Met (78/3%)
Asn-335/Asn-337/Glu-327	Asn (2,101/80%)	Glu (10/0.38%)

[a] Distribution of the 5 candidate residues of mthAK/ATP-ecoAK/PPi-ehiAK (Asn-211/Asn-213/Thr-201, Ala-330/Gly-332/Asp-322, Gly-331/Gly-333/Gln-323, Ile-332/Ile-334/Met-324, and Asn-335/Asn-337/Glu-327) in a database search of AKs. A total of 2,625 PPi-ehiAK homologs were found using BLASTP (25) on the GenomeNet server (http://www.genome.jp). [b] Number and percentage (%) of PPi-ehiAK homologs possessing the indicated amino acid at the position of the candidate residue.

Supplementary information

Table S1. Interactions between mthAK and ADP [a]

Hydrogen bonds				van der Waals contacts		
ADP atoms	Target atoms	Distance (Å)	ADP atoms	Target atoms	Distance (Å)	
β-phosphate						
O2B	Asn-211[b]	N	2.7			
O3B	Gly-331[b]	N	2.6			
Ribose						
O2'	Phe-284[c]	N	3.3	C1'	Gly-331[b]	C	3.7
O3'	Asp-283[c]	OD2	3.3		Ile-332[b]	CG1	3.5
O4'	Ile-332[b]	N	3.6	C2'	Phe-284[c]	CB	3.9
Adenine						
N3	Arg-285[c]	N	3.5	C2	Arg-285[c]	CA	3.6
N6	Asn-335[b]	O	3.4			CB	3.9
	Arg-362[d]	NH_2	3.2		Ser-336[d]	CB	3.8
N7	Asn-335[b]	ND2	3.2	C5	Asn-335[b]	CB	3.8
N9	Gly-331[b]	O	3.4				

[a] Interactions between ADP and residues of mthAK B chain. [b] Five candidate residues specific to PPi-ehiAK. [c] Five residues conserved in mthAK, ATP-ecoAK, and PPi-ehiAK. [d] Residues not conserved.

Table S2. AK activity in the PPi-forming direction using Pi as a phosphoryl acceptor [a].

Enzyme	PPi (μM)
PPi-ehiAK	3.1
ATP-ecoAK	nd [b]
ATP-ecoAK N213T	nd
ATP-ecoAK G332D	nd
ATP-ecoAK G333Q	nd
ATP-ecoAK I334M	nd
ATP-ecoAK N337E	nd

[a] AK activity in the PPi-forming direction was assayed as described in the Materials and Methods. After reaction for 20 min with 1.4×10^{-2} μg of PPi-ehiAK, the reaction mixture was diluted 50-fold with distilled water and RLU was measured. PPi at 1.0 μM gave ΔRLU of 955,937. nd, not detected.

[b] ΔRLU was zero with 9.2, 3.1, 2.4, 5.8, 2.9, and 3.1 μg of ATP-ecoAK, ATP-ecoAK N213T, ATP-ecoAK G332D, ATP-ecoAK G333Q, ATP-ecoAK I334M and ATP-ecoAK N337E, respectively, after the reaction for 20 min; thus, AK activities in the PPi-forming direction of ATP-ecoAK and these mutated ATP-ecoAKs using PPi were regarded as not detected (nd).

Table S3. Residues interacting with Thr-201 and Asp-322 in PPi-ehiAK[a].

	Hydrogen bonds			van der Waals contacts			
	Target atoms		Distance (Å)		Target atoms		Distance (Å)
Thr-201							
O	Gly-202[b]	N	3.4				
Asp-322							
O	Leu-326[c]	N	3.4				
OD1	His-198[b]	ND1	3.3	CA	Asn-376[c]	CG	3.9
		NE2	2.3	CB	Leu-199[b]	C	3.4
OD2	Leu-199[b]	O	3.6		Gly-200[b]	CA	3.9
	Gly-200[b]	N	3.3	CG	Leu-199[b]	C	3.9
N	Asn-376[c]	OD1	3.1		Gly-200[b]	CA	3.4

[a] The residues interacting with Thr-201 and Asp-322 in PPi-ehiAK. Thr-201 and Asp-322 are expected to be around the phosphate group. [b] Four residues conserved in the primary structures of mthAK, ATP-ecoAK, and PPi-ehiAK. [c] Two residues conserved in ATP-dependent AKs, but not in PPi-ehiAK. This is the reason why we focused on these residues (Leu-326 and Asn-376 in PPi-ehiAK).

Table S4. Distribution of the 5 candidate residues.

Homolog name	Species name	Amino-acid residue corresponding to				
		Glu-327	Thr-201	Asp-322	Gln-323	Met-324
		of PPi-ehiAK				
EDI_237080 [a]	*Entamoeba dispar*	Glu	Thr	Asp	Gln	Met
GM21_0328 [a]	*Geobacter* sp. M21	Glu	Asn	Tyr	Gly	Glu
Gbem_0348 [a]	*Geobacter bemidjiensis*	Glu	Asn	Tyr	Gly	Glu
GM18_0425 [a]	*Geobacter* sp. M18	Glu	Asn	Tyr	Gly	Glu
Tpet_1041 [a]	*Thermotoga petrophila*	Glu	Ser	Gly	Gly	Met
Tnap_1061 [a]	*Thermotoga naphthophila*	Glu	Ser	Gly	Gly	Met
TRQ2_1071 [a]	*Thermotoga* sp. RQ2	Glu	Ser	Gly	Gly	Met
Tmari_1762 [a]	*Thermotoga maritima*	Glu	Ser	Gly	Gly	Met
TM1754 [a]	*Thermotoga maritima*	Glu	Ser	Gly	Gly	Met
ATP-ecoAK [a, b]	*E. coli*	Asn	Asn	Gly	Gly	Ile
mthAK	*M. thermophila*	Asn	Asn	Ala	Gly	Ile

[a] Proteins in KEGG database (http://www.genome.jp/kegg/).

[b] Y75_p2262 in KEGG database.

CGCGCGGCAGCCATATGTCTAATGTGCTGATTTTCAACGTAGGATCTAGTTCCCTCACATATAAA
GTGTTTTGTAGCGACAACATCGTCTGTAGTGGCAAATCCAATCGCGTGAATGTGACTGGTACTG
AGAAACCGTTTATCGAACATCACTTAAACGGCCAAATCATTAAGATAGAAACCCCAATCCTCAA
CCATCCACAGGCTGCAAAACTGATTATCCAGTTCCTGAAAGAGAACCACATCTCTATTGCCTTT
GTAGGCCATCGCTTTGTTCATGGCGGGTCTTACTTTAAGAAATCAGCCGTCATTGACGAAGTCG
TGCTGAAAGAACTGAAAGAATGCCTGCCTTTAGCGCCCATTCATAACCCGAGCTCTTTCGGAG
TTATCGAAATCTCGATGAAAGAACTGCCAACCACTCGTCAGTATGTGGCGATCGATACGGCGTT
CCATTCGACCATTTCCCAAGCTGAACGCACCTATGCGATTCCGCAGCCGTATCAATCGCAGTAT
CTGAAATTCGGCTTTCACGGCCTGTCATACGAATACGTGATCAACTCGTTGAAGAATGTCATTG
ACGTAAGTCACAGCAAAATCATTGCATGCCATCTTGGTACAGGTGGCTCCTCATGCTGCGGCAT
TGTGAATGGGAAATCGTTTGATACGAGTATGGGTAACAGCACACTTGCTGGTCTGGTGATGTCA
ACGCGTTGTGGGGATATTGATCCCACCATTCCGATTGATATGATCCAGCAAGTGGGTATTGAGA
AAGTTGTCGATATTCTCAACAAGAAAAGCGGCTTGCTTGGGGTCAGTGAACTGAGCAGCGATA
TGCGCGATATTTTGCACGAAATCGAAACCCGTGGTCCTAAAGCCAAAACGTGCCAACTGGCCT
TTGATGTTTACATCAAACAGCTGGCGAAAACCATCGGAGGCCTGATGGTTGAGATCGGCGGTC
TTGACTTACTGGTGTTCACCGATCAGATGGGTCTGGAAGTATGGCAAGTTCGGAAAGCGATATG
CGACAAAATGAAATTTCTGGGCATTGAGTTGGACGATAGCCTCAATGAGAAGTCCATGGGTAA
GAAAATTGAATTCCTGACGATGCCGAGCAGCAAGGTACAGGTTTGTGTTGCACCGAATGACGA
GGAATTAGTCATACTGCAGAAAGGGAAAGAATTATTCCAGTTTTAACTCGAGCACCACCACC

Fig. S1. The sequence of *PPi-ehiAK* with optimized codon usage for *E. coli*. The optimized PPi-ehiAK gene (KEGG ID; ehi: EHI_170010) was synthesized at Operon. The *Nde*I site (CATATG) and *Xho*I site (CTCGAG) are underlined. The start codon (ATG) and stop codon (TAA) are shown in bold.

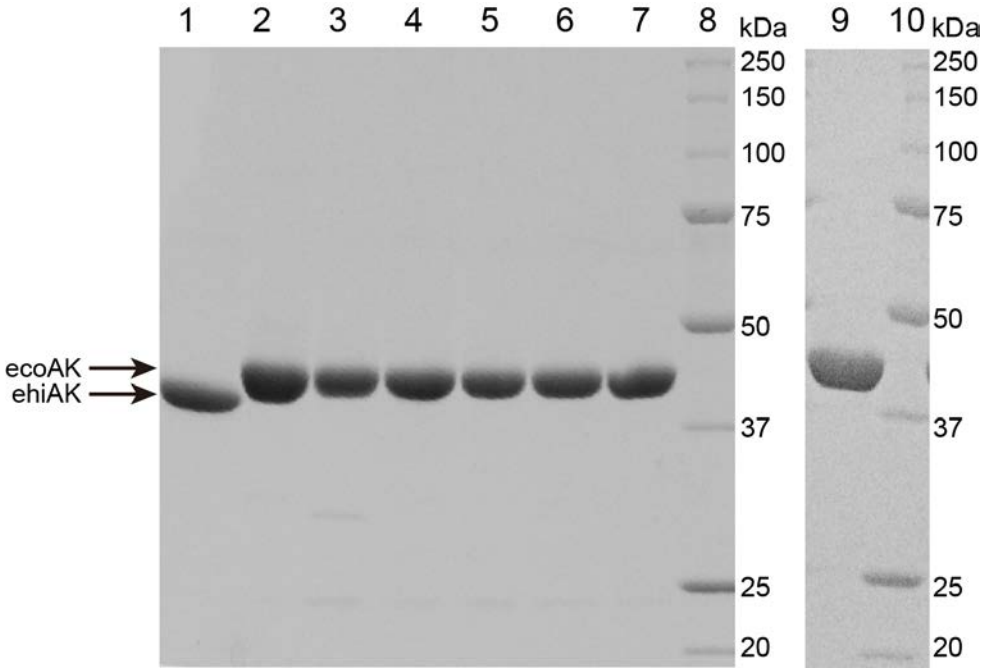

Fig. S2. SDS-PAGE of purified AKs. Lanes 1–7, 9: purified PPi-ehiAK, ATP-ecoAK, ATP-ecoAK N213T, ATP-ecoAK G332D, ATP-ecoAK G333Q, ATP-ecoAK I334M, ATP-ecoAK N337E, and ATP-ecoAK N213T G332D E336L T385N (5.0 μg). Arrows indicate positions of purified AKs. Lanes 8 and 10: protein markers (Bio-Rad Laboratories, Hercules, CA).

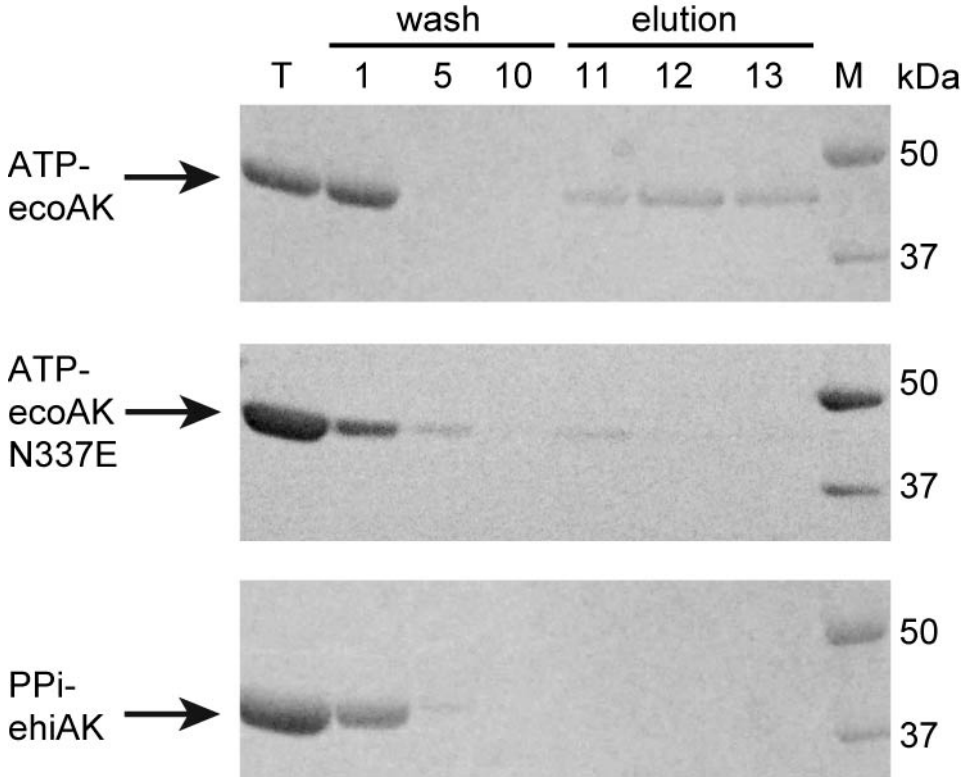

Fig. S3. SDS-PAGE of AKs eluted from an ATP-agarose column. Lane T: flow-through fraction; Lanes 1, 5, and 10: Fractions washed with 10 mM Tris-HCl (pH 8.0) containing 10 mM $MgCl_2$ or 20 mM HEPES-NaOH (pH 7.5) containing 10 mM $MgCl_2$; Lanes 11, 12, and 13: Fractions eluted with 50 mM ATP containing 10 mM $MgCl_2$; Lane M: protein markers. Lane numbers correspond to the numbers of fractions (200 µL each). Arrows indicate the positions of AKs.

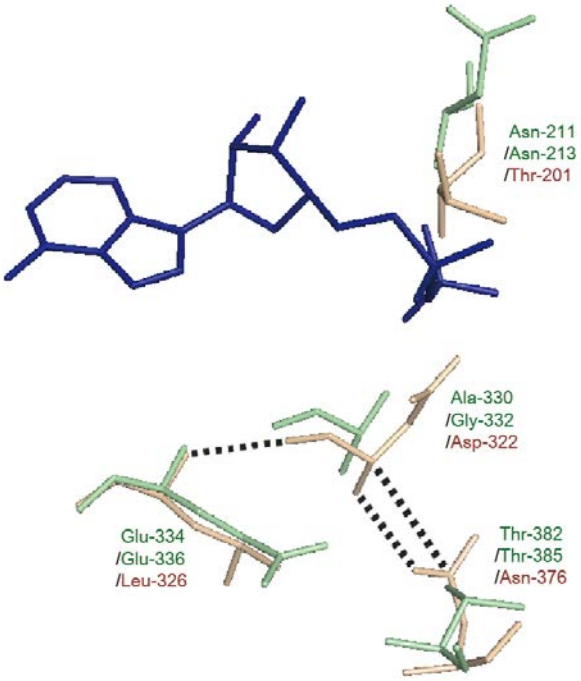

Fig. S4. Superposition of mthAK and PPi-ehiAK around the phosphate group of ADP. Superposition of the tertiary structure of PPi-ehiAK (PDB, 4H0O) (1) and that of mthAK complexed with acetate and ADP-AlF_3 (PDB, 1TUY) (2). Amino acid residues of mthAK are shown in green; ADP in mthAK is in deep blue, and PPi-ehiAK is in light orange. The residue names and numbers are shown for mthAK (green)/ATP-ecoAK (green)/PPi-ehiAK (pink). Hydrogen bonds in PPi-ehiAK are shown as dashed lines. Superposition of AKs was performed using PyMOL.

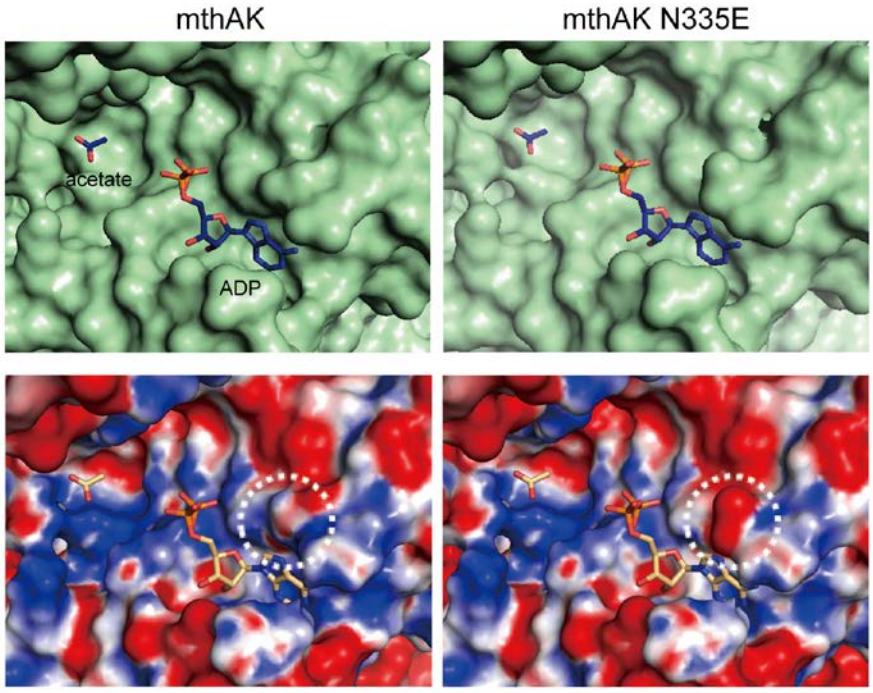

	mthAK	mthAK N335E
K_m (mM)	0.67 ± 0.06	30.7 ± 1.9
V_{max} (U/mg)	1,258 ± 28	537 ± 24

Fig. S5. ADP-binding sites of mthAK and mthAK N335E. Molecular surfaces of ADP-binding sites of mthAK (left) and mthAK N335E (right) are shown in the upper panels. Electrostatic surfaces of the AKs are shown in the lower panels. Positive and negative charges at pH 7.0 are colored in blue and red, respectively, and were calculated using APBS (3). The position around Asn-335 is denoted by a white dotted circle. K_m and V_{max} for ATP of ATP-ecoAK and ATP-ecoAK N337E are shown under the respective figures.

References

1. **Thaker, T. M., Tanabe, M., Fowler, M. L., Preininger, A. M., Ingram-Smith, C., Smith, K. S., and Iverson, T. M.:** Crystal structures of acetate kinases from the eukaryotic pathogens *Entamoeba histolytica* and *Cryptococcus neoformans*, J. Struct. Biol., **181**, 185-189 (2013).
2. **Gorrell, A., Lawrence, S. H., and Ferry, J. G.:** Structural and kinetic analyses of arginine residues in the active site of the acetate kinase from *Methanosarcina thermophila*, J. Biol. Chem., **280**, 10731-10742 (2005).
3. **Baker, N. A., Sept, D., Joseph, S., Holst, M. J., and McCammon, J. A.:** Electrostatics of nanosystems: application to microtubules and the ribosome, Proc. Natl. Acad. Sci. USA., **98**, 10037-10041 (2001).